Image Models and Their Role in Image Processing. Some Multichannel Results.

Rafael Molina and Javier Mateos
Departamento de Ciencias de la Computación e Inteligencia Artificial
Universidad de Granada.
18071 Granada. España.

Abstract

Over the last few years an enormous amount of research has been devoted to restore astronomical images, but not much work has been reported on the use of multichannel techniques to restore such images.

In this work, we first briefly summarize the research carried out on image restoration within the *Converging Computing Methodologies* network and then concentrate on the multichannel image restoration problem, a field we believe of interest to the astronomical community.

The Bayesian paradigm to restore multichannel astronomical images is described and multichannel image restoration methods are adapted to the Poisson noise degradation model. The methods are compared on real multichannel astronomical images.

1 Introduction

According to [1] the field of image restoration began primarily with the efforts of scientists involved in the space programs of both the United States and the former Soviet Union in the 1950s and early 1960s. Also, the discovery of the spherical aberration problem in the Hubble Space Telescope in 1990 led to a very substantial amount of work in image restoration and reconstruction directed toward optical Astronomy. These two reasons probably explain the enormous interest on image restoration techniques within the astronomical community.

Very recently, we have seen the publication of two excellent works on image restoration and reconstruction [1, 14] which constitute invaluable references for those researchers involved in image restoration and in particular in image restoration in Astronomy.

Within the European Science Foundation network *Converging Computing Methodologies in Astronomy* quite a lot of effort has been devoted to work on the image restoration problem. A proof of that are the papers presented at the first workshop of the network held in Nice in 1995 [2], where works on edge preserving restoration methods [3], the application of Compound Gauss-Markov Random Fields to astronomical image restoration [11], spatially adaptive reconstruction methods [15], multiresolution techniques based in wavelets [16] and finally multiscale maximum entropy methods [20] were presented.

The third workshop of the CCMA network took place last April in Granada and was devoted to Information Fusion and Data Mining [13], and works on simultaneous image fusion and reconstruction using wavelets [17] and multichannel image restoration [12] were presented.

In spite of the interest in image restoration, to our knowledge no much work has been devoted within the astronomical community to the multichannel restoration problem. However, the use of image data from multiple frequency bands, multiple time frames, or multiple sensors can be of tremendous value in a number of applications, such as multispectral satellite remote sensing, multisensor robot guidance, multimedium medical diagnosis and obviously astronomical image restoration.

Multichannel image processing differs from single channel image processing because of the redundancy and the complementary feature of information within channels. The processing is much more complicated due to the increased dimension and the need for extracting and exchanging information from and among all channels.

Single channel restoration has been researched extensively during the past couple of decades [10, 14]. Multispectral and multichannel restoration are relatively new areas of image processing research. Decorrelation of the image channels using the Karhunen-Loeve transform [9] has been used prior to restoring the channels individually. Extending linear methods such as Wiener filtering [5] and least squares restoration [6] has been accomplished successfully, although the accurate estimation of nonstationary cross-channel correlations remains elusive.

Recently multispectral image model for use in Bayesian maximum a posteriori estimation have been proposed (see [19] and [4]). In these works the Gibbs priors contain spatial and spectral cliques functions to impose constrains on the desired restoration or

segmentation.

In our previous work [12] we presented some work on multichannel techniques for the Gaussian independent noise model. In this work we extend our results to the Poisson noise model and show how the method work on real astronomical images.

In this paper we present the application of the Bayesian paradigm to the restoration of multichannel images. In section 2 we introduce the paradigm we follow. The degradation model we use in the paper is described in section 3. In section 4 we examine existing image models to restore multichannel images. In section 5 we describe an iterative method that can be used to find the multichannel restoration. Finally, a comparative study of the methods used is performed in section 6.

2 Bayesian Paradigm

We will distinguish between f, the 'true' image which would be observed under ideal conditions (i.e. no noise and no distortions produced by blurring and instrumental effects), and g, the observed image. The aim is then to reconstruct f from g. Bayesian methods start with a *prior distribution*, a probability distribution over images f. It is here where we incorporate information on the expected structure within an image. It is also necessary to specify $p(g|f)$, the probability distribution of observed images g if f were the 'true' image. The Bayesian paradigm dictates that inference about the true f should be based on $p(f|g)$ given by

$$p(f|g) = p(g|f)p(f)/p(g) \propto p(g|f)p(f). \tag{1}$$

To show just one restoration it is common (but not obligatory) to choose the mode of $p(f|g)$, that is, to display the image $\hat{f}$ which satisfies

$$\hat{f} \text{ maximizes } p(g|f)p(f). \tag{2}$$

This is known as the MAP (maximum a posteriori) estimate of f.

Let us now examine the degradation and image models.

3 Degradation Model

Let us assume for simplicity we have three channels, each of them with $p = M \times N$ pixels, then we have

$$g = \begin{pmatrix} g_1 \\ g_2 \\ g_3 \end{pmatrix}, \qquad f = \begin{pmatrix} f_1 \\ f_2 \\ f_3 \end{pmatrix}, \tag{3}$$

where each of the $M \times N$ vectors g_i, f_i results from the lexicographic ordering of the two-dimensional signals in each channel. We will denote by $f_i(u)$ the intensity of the true channel i image at the location of the pixel u on the lattice. The convention applies equally to the observed image g.

For the degradation model we assume Poisson noise with no cross channel degradation, that is

$$p(g|f) = \prod_{i=1}^{3} \prod_{u=1}^{p} \exp\left[-(H_i f_i)(u)\right][(H_i f_i)(u)]^{g_i(u)}/g_i(u)!\,, \tag{4}$$

where H_i, $i = 1, 2, 3$, represents the blurring matrix within each channel.

4 Image Models

In this section we describe some image models that can be used in the multichannel restoration problem. Not all of them will be compared in the test section, but we intend to provide a summary of some image models that could be used for multichannel image restoration in Astronomy.

4.1 CAR model without cross channel information. Model I

Let us first describe the prior model without cross-channel information. Our prior knowledge about the smoothness of the object within each channel makes it possible to model the distribution of f_i, for $i = 1, 2, 3$, by a Conditional Autoregressive Model (CAR) (see Ripley [18]). Thus,

$$p(f_i) \propto \exp\left\{-\gamma_i f_i^T (I - C) f_i\right\}, \tag{5}$$

where $C_{uv} = 0.25$ if cells u and v are spatial neighbors (pixels at distance one), zero otherwise. The term $f_i^T(I - C)f_i$ represents in matrix notation the sum of squares of the values $f_i(u)$ minus 0.25 times the sum of $f_i(u)f_i(v)$ for neighboring pixels u and v. The parameter γ_i measures the smoothness of the 'true' channel i image.

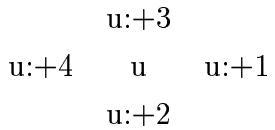

Figure 1: Image sites at each channel.

From Eq. 5 we have

$$p(f_i) \propto \exp[-\frac{\alpha_i}{2}\sum_u[(f_i(u) - f_i(u:+1))^2 + (f_i(u) - f_i(u:+2))^2]], \tag{6}$$

where $u:+1$, $u:+2$, $u:+3$, $u:+4$ denote the four pixels around pixel u as described in figure 1, $\alpha_i = 0.5\gamma_i$ and we assume a 'toroidal edge correction'.

Before describing the models used in the paper, it is very important to note that although in [6] and [7] the methods used are based on Laplacians and so they can be considered as setting constrains on second derivatives we are going to formulate them as methods based on CAR models and so as methods that set constrains on first derivatives.

4.2 Model proposed by Guo, Lee and Teo. Model II.

Although the method proposed in [7] is based on the $3D$ Laplacian and so it could be considered as a Simultaneous Autoregressive Model (SAR), we can easily find its Conditional Autoregressive version. This is given by

$$\begin{aligned} p(f) \propto \quad & \exp[-\frac{\alpha_{12}}{2} \parallel f_1 - f_2 \parallel^2 - \frac{\alpha_{23}}{2} \parallel f_2 - f_3 \parallel^2 - \frac{\alpha_{13}}{2} \parallel f_1 - f_3 \parallel^2] \\ & \prod_{i=1}^{3} \exp[-\frac{\alpha_i}{2}\sum_u[(f_i(u) - f_i(u:+1))^2 + (f_i(u) - f_i(u:+2))^2]], \end{aligned} \tag{7}$$

where $\parallel f_i - f_j \parallel^2 = \sum_u (f_i(u) - f_j(u))^2$. It is very important to note that this model does not normalize each channel and so the square differences involved in the prior may not have much sense. A similar model is used in [8] for medical images.

4.3 Model proposed by Galatsanos, Katsaggelos, Chin and Hillery. Model III.

This method was proposed before the one described in [7] and it takes into account the norm of each channel. The CAR model is given by Eq. (7) but f_i is replaced by $f_i / \parallel f_i \parallel$.

4.4 Model proposed by Molina and Mateos. Model IV.

One of the problems with models II and III is that they do not keep the flux within each channel. For the degradation model described by Eq. (4) it makes perfect sense to try to keep the flux within each channel. To achieve so we simply replace f_i in Eq. (7) by $f_i/(\sum_u f_i(u))$, see [12].

4.5 Model proposed by Schultz and Stevenson. Model V.

The model proposed in [19] uses 8-neighbors within each channel and instead of using the quadratic edge penalty $\rho(x) = x^2$ uses a Huber-Markov Random Field to model each channel spatially.

Spatial activity measures, the difference between neighbor pixels in each channel, will be used as edge detectors within each channel. Weighted differences of these spatial activity measures are used as the spectral clique functions, with weights estimated to account for edges in one channel that are not present in another (see [19] for details).

4.6 Other Models

It is important to note that the penalty function $\rho(x) = x^2$ can be substituted by other functions. In particular, we can use

$$\rho(x) = x^2/(\delta^2 + x^2) \quad \text{and} \quad \rho(x) = \log(1 + (x/\mu)^2).$$

It is also possible to use models based on estimating the cross-channel correlation from the data [5]. It is important to note that [5] contains interesting results on the use of Fourier transform to solve the multichannel problem.

5 Iterative Procedure

In this section we describe a simple iterative method that can be used to restore multichannel astronomical images. It will be described for model II, but it can also be applied to models III and IV if either $\| f_i \|$ or $\sum_u f_i(u)$, $i = 1, 2, 3$, are assumed constant.

Assuming image model II, we have

$$p(f|g) \quad \propto \quad \exp[-\alpha_{12} \| f_1 - f_2 \|)^2 - \alpha_{23} \| f_2 - f_3 \|)^2 - \alpha_{13} \| f_1 - f_3 \|)^2]$$

$$\times \prod_{i=1}^{3} \exp[-\alpha_i \sum_u [(f_i(u) - f_i(u:+1))^2 + (f_i(u) - f_i(u:+2))^2]$$
$$\times \prod_{i=1}^{3} \prod_{u=1}^{p} \exp\left[-(H_i f_i)(u)\right][H_i f_i)(u)]^{\mathbf{g}_i(u)}/g_i(u)!\,.$$

Differentiating $-\log p(f|g)$ with respect to f_1, the same can be done for f_2 and f_3, we have

$$\alpha_1(I - C)f_1 + \alpha_{12}(f_1 - f_2) + \alpha_{13}(f_1 - f_3) + \mathbf{1} - H_1^t(g_1/H_1 f_1) = 0, \tag{8}$$

where $\mathbf{1}$ denotes the $p \times 1$ vector with each component equal to 1.

From Eq. (8) we have

$$(\alpha_1 + \alpha_{12} + \alpha_{13})f_1 + \mathbf{1} = \alpha_1 C f_1 + \alpha_{12} f_2 + \alpha_{13} f_3 + H_1^t(g_1/H_1 f_1), \tag{9}$$

multiplying both sides of Eq. (9) by f_1 we obtain the following iterative scheme,

$$f_1^{j+1}(u) = \mu_1(u)[C f_1^j](u) + \mu_2(u) f_1^j(u)[H_1^t(g/H_1 f_1^j)](u) + \mu_3(u) f_2^j(u) + \mu_4(u) f_3^j(u), \tag{10}$$

where, j denotes iteration and

$$\begin{aligned}
\mu_1(u) &= \alpha_1 f_1^j(u)/((\alpha_1 + \alpha_{12} + \alpha_{13})f_1^j(u) + 1), \\
\mu_2(u) &= 1/((\alpha_1 + \alpha_{12} + \alpha_{13})f_1^j(u) + 1), \\
\mu_3(u) &= \alpha_{12} f_1^j(u)/((\alpha_1 + \alpha_{12} + \alpha_{13})f_1^j(u) + 1), \\
\mu_4(u) &= \alpha_{13} f_1^j(u)/((\alpha_1 + \alpha_{12} + \alpha_{13})f_1^j(u) + 1),
\end{aligned}$$

6 Test Examples

The models I to IV were tested on the multichannel astronomical images shown in figure 2(a)-(c). They correspond to images of the same object taken at different wavelength. The range for each image is $[0, 10]$ for figure $2a$, $[0, 24]$ for figure $2b$ and $[0, 62]$ for figure $2c$.

The blurring function, h_i can be approximated by $h_i(r) \propto (1 + r^2/R^2)^{-\delta}$, $i = 1, 2, 3$. We found $\delta \sim 3$ and $R \sim 3.4$ pixels in all the channels.

For model I we used $\alpha_1 = \alpha_2 = \alpha_3 = 0.0035$. For model II we used $\alpha_1 = \alpha_2 = \alpha_3 = 0.0035$ and $\alpha_{12} = \alpha_{13} = \alpha_{23} = 0.0035$. For model III we used $\alpha_1 = \alpha_2 = \alpha_3 = 1$ and $\alpha_{12} = \alpha_{13} = \alpha_{23} = 1$. For model IV we used $\alpha_1 = \alpha_2 = \alpha_3 = 0.013$ and $\alpha_{12} = \alpha_{13} = \alpha_{23} = 0.013$.

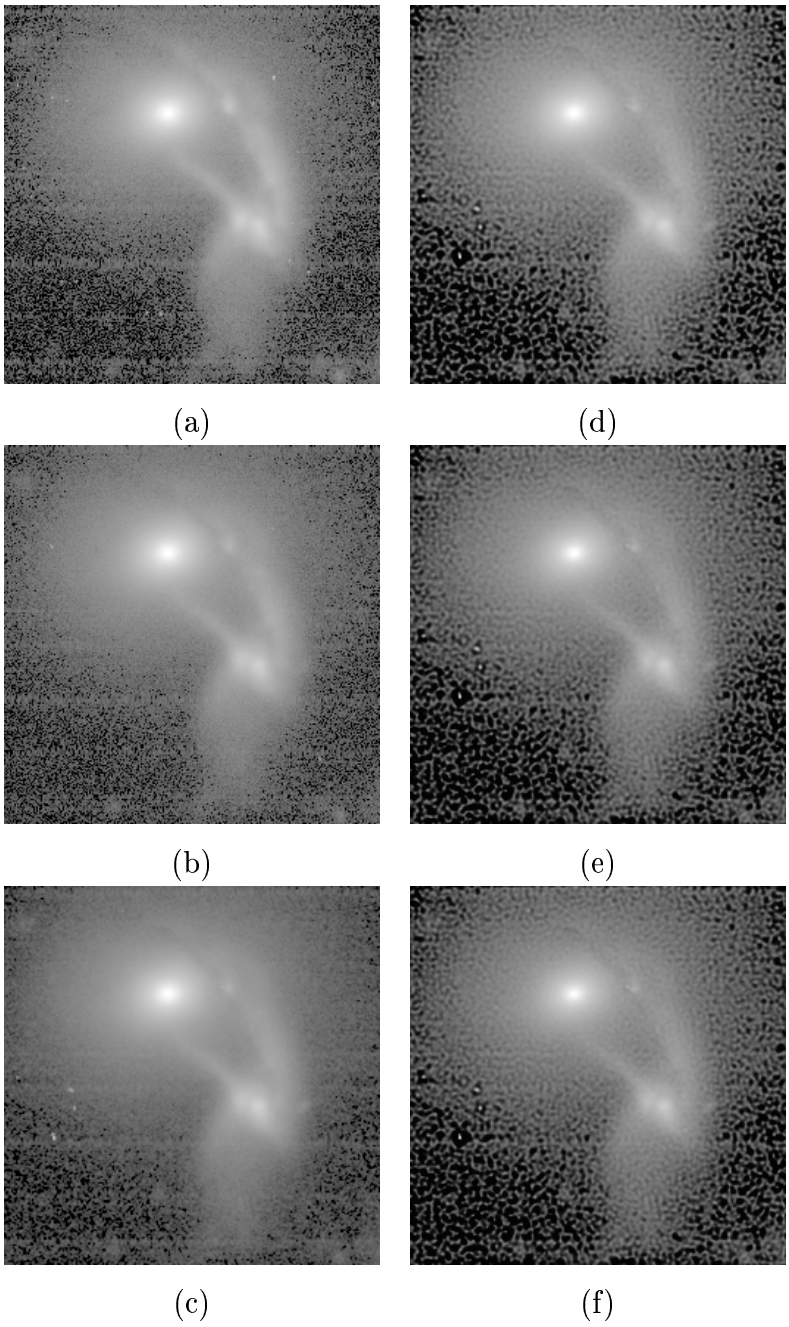

Figure 2: Observed image at three different wavelength corresponds to (a), (b) and (c). (d) Restoration of (c) using model II. (e) Restoration of (c) using model III and (f) Restoration of (c) using model IV.

image	original	Model I	Model II	Model III	Model IV
Figure 2a	10	13	16	13	13
Figure 2b	24	31	23	30	32
Figure 2c	62	79	53	76	87

Figure 3: Maximum values of the observed and restored images.

These values for the parameters were choosen based on the scale factor used by each method on each band.

Figure 3 shows the maximum values of each observed image and the corresponding restorations.

From the experiments we have run we have found that model II moves a lot of flux between channels, In our examples increases enormously the flux of image in figure 2a and reduces the other ones. Models I, III and IV produce similar results but model IV seems to produce better restorations maximum values. Models I and IV are the only ones that keep the flux within each channel.

Acknowledgments

We would like to thank A. del Olmo and J. Perea, members of the Instituto de Astrofísica de Andalucía, for providing us with the images we have used in this paper.

References

[1] M. R. Banham and A.K. Katsaggelos, "Digital Image Restoration", IEEE Signal Processing Magazine, vol. 14, no. 2, pp. 24-41, 1997.

[2] A. Bijaoui, *Vision Modeling and Information Coding*, Special issue of *Vistas in Astronomy*, vol. 40, no. 4, 1996.

[3] L. Blanc-Feraud and M. Barlaud ,"Edge Preserving restoration Techniques", *Vistas in Astronomy*, vol. 40, no. 4, pp. 531-538, 1996.

[4] M.M. Chang, M.I. Sezan, A.M. Tekalp and M.J. Berg,"Bayesian segmentation of multislice brain magnetic resonance imaging using three-dimensional Gibbsian priors", *Optical Engineering*, vol. 35, no. 11, pp. 3206–3221, 1996.

[5] N.P. Galatsanos and R.T. Chin, "Digital Restoration of Multichannel Images", *IEEE Trans. Acoust., Speech, Signal Processing*, vol. 37, no. 3, pp. 415–421, 1989.

[6] N.P. Galatsanos, A.K. Katsaggelos, R.T. Chin and A.D. Hillery, "Least Squares Restoration of Multichannel Images", *IEEE Trans. on Signal Processing*, vol. 39, no. 10, pp. 2222–2236, 1991.

[7] Y.P. Guo, H.P. Lee and C.L. Teo, "Multichannel Image Restorations Using Iterative Algorithm in Space Domain", *Image and Video Computing*, vol. 14, pp. 389–400, 1996.

[8] T. Hebert and R. Leahy, "A generalized EM algorithm for 3-D Bayesian Reconstruction from Poisson Data Using Gibbs Priors", *IEEE Trans. on Medical Imaging*, vol. 8, no. 2, pp. 194-202, 1989.

[9] B.R. Hunt and O. Kübler, "Karhunen-Loeve multispectral image restoration, part 1: Theory", *IEEE Trans. Acoust., Speech, Signal Processing*, vol. 32, no. 3, pp. 592–600, 1984.

[10] Katsaggelos, A.K., editor, *Digital Image Restoration*, Springer Series in Information Sciences, vol. 23, Springer-Verlag, 1991.

[11] R. Molina, A.K. Katsaggelos, J. Mateos and J. Abad, "Compound Gauss-Markov Random Fields for Astronomical Image Restoration", *Vistas in Astronomy*, vol. 40, no. 4, pp. 539-546, 1996.

[12] R. Molina, R. and J. Mateos, Multichannel Image Restoration in Astronomy, to appear in *Vistas in Astronomy*, 1997.

[13] R. Molina, F. Murtagh and A. Heck , *From Information Fusion to Data Mining*, Special issue of *Vistas in Astronomy* to appear.

[14] J. Nuñez, (editor), *Image Reconstruction and Restoration in Astronomy*, Special issue of *International Journal of Imaging Systems and Technology* , vol. 6, no. 4, 1995.

[15] J. Nuñez and J. LLacer, "Image Reconstruction with Variable Resolution Using Gaussian Invariant Functions in a Segmentation Process", *Vistas in Astronomy*, vol. 40, no. 4, pp. 547-554, 1996.

[16] J. Nuñez and X. Otazu, "Multiresolution Image Reconstruction Using Wavelets", *Vistas in Astronomy*, vol. 40, no. 4, pp. 555-562, 1996.

[17] J. Nuñez, X. Otazu, O. Fors and A. Prades, "Simultaneous Image Fusion and Reconstruction using Wavelets. Applications to SPOT+LANDSAT Images", to appear in *Vistas in Astronomy*, .

[18] B.D. Ripley (1981)"Spatial Statistics", Wiley, New York.

[19] R.R. Schultz and R.L. Stevenson, "Stochastic Modeling and Estimation of Multispectral Image Data", *IEEE Trans. on Image Processing*, vol. **IP**4, no. 8, pp. 1109–1119, 1995.

[20] J-L. Starck and E. Pantin, "Multiscale maximum Entropy Image Restoration", *Vistas in Astronomy*, vol. 40, no. 4, pp. 563-570, 1996.